

Ultra-High-Temperature Ceramic Matrix Composites for Hybrid Rocket Nozzles

Giuseppe D. Di Martino^{a*}, Stefano Mungiguerra^a, Anselmo Cecere^a, Raffaele Savino^a,
Luca Zoli^b, Antonio Vinci^b, Laura Silvestroni^b, Diletta Sciti^b

^a *University of Naples “Federico II”, Department of Industrial Engineering, Aerospace Division, P.le Tecchio 80, 80125 Napoli, Italy*

^b *National Research Council of Italy, Institute of Science and Technology for Ceramics, Via Granarolo 64, 48018 Faenza, Italy*

* Corresponding Author, e-mail: giuseppedaniele.dimartino@unina.it

Abstract

This paper presents the results of the activities carried out in the framework of the Horizon 2020 project C³HARME aimed at characterizing a new class of Ultra-High-Temperature Ceramic Matrix Composites (UHTCMC) for application as hybrid rocket nozzle. The material is based on a ZrB₂-SiC matrix reinforced with either short or long carbon fibres. An incremental approach has been adopted for the material characterization, in terms of test articles dimensions and geometrical complexity. In particular, a first screening of the most suitable materials candidates has been performed testing small button-like specimens exposed to the supersonic exhaust jet of a 200N-class hybrid rocket nozzle. Based on the results, flat disks to be placed inside the hybrid rocket combustion chamber were manufactured and tested to assess the capability of larger components to withstand the thermo-mechanical stresses expected inside the rocket. Finally, nozzle throat inserts and complete subscale nozzles were tested, comparing their behaviour to a classical graphite nozzle tested in the same operating conditions. Results showed that long fibers materials with optimised porosity level have strong mechanical properties and outstanding erosion resistance.

Keywords: Ultra-High-Temperature Ceramic Matrix Composites; ZrB₂-SiC; hybrid rocket; rocket nozzles

Acronyms/Abbreviations

| | |
|--------|--|
| CI | Chamber insert |
| CN | Complete nozzle |
| FJ | Free jet |
| HDPE | High Density Polyethylene |
| ISTEC | Institute of Science and Technology for Ceramics |
| LF | Long fibers |
| SF | Short fibers |
| TI | Nozzle throat insert |
| UHTC | Ultra-High-Temperature Ceramics |
| UHTCMC | Ultra-High-Temperature Ceramic Matrix Composite |
| UNINA | University of Naples “Federico II” |

1. Introduction

One of the most challenging requirements in rocket engine design is that dimensional stability of the nozzle throat should be maintained guaranteeing a stable engine operation, which makes the selection of rocket nozzle materials extremely hard. In fact, very high shear stresses and heat fluxes are typically encountered on the inner surface of high performance rocket nozzles, where the propellant flow is accelerated to supersonic conditions. These severe conditions, combined to the high pressure and the chemically aggressive environment, usually lead to removal of surface material

due to heterogeneous reactions between oxidizing species in the hot gas and the solid wall [1, 2].

The materials used for these applications include refractory metals, refractory metal carbides, graphite, ceramics and fiber-reinforced plastics [3, 4]. Certain classes of materials demonstrated superior performances under specific operating conditions but the choice depends on the specific application. For instance, fully densified refractory-metal nozzles generally are more resistant to erosion and thermal-stress cracking than the other materials. Graphite performs well with the least oxidizing propellants but is generally eroded severely [5, 6, 7].

In recent years, Ultra-High-Temperature Ceramic (UHTC) materials, including zirconium or hafnium diborides or carbides, are gaining an increasing importance because of their unique high temperature properties, such as high melting points, temperature strength and oxidation resistance, which allow them to survive the extreme environments encountered in the rocket propulsion environment. Some of these materials proved to be very interesting to develop aerospace components working in harsh environments [8, 9, 10]. Bulk UHTCs with addition of silicon based ceramics, in the form of particles, short fibers or whiskers have been developed with good oxidation and ablation resistance at ultra-high temperature [11, 12]. However, the

application of single phase materials, without secondary phases, is limited by characteristics such as low fracture toughness, low thermal shock resistance and lack of damage tolerance. Therefore, composites with continuous carbon fibers as reinforcement and UHTC or C/SiC-UHTC as matrix can be expected to perform good erosion resistance properties compared to C/C and C/SiC composites, as well as good thermal shock resistance and damage tolerance [13, 14, 15] and then to be the potential candidates for use in propulsion applications.

This so-called Ultra High Temperature Ceramic Matrix Composites (UHTCMC), are the subject of the Horizon 2020 European C³HARME research project, focused on materials design and preparation, development of components from small to larger scale and testing in representative environments, including both solid and hybrid rocket nozzles [16].

In this work, the results of the activities carried out for the characterization of the new-class UHTCMCs in for application in hybrid rocket are presented and discussed. Experimental tests are performed employing a 200N-class hybrid rocket operated with gaseous oxygen burning cylindrical port High-Density PolyEthylene (HDPE) fuel. The experimental activities were divided in different steps, following an incremental approach in terms of sample dimensions and prototype geometrical complexity. Non-intrusive diagnostic equipment, including two-color pyrometers and an infrared thermo-camera, has been employed to monitor the surface temperature of the samples that reached values over 2800 K.

2. Experimental facility and setup

The experimental activities presented in this work have been carried out at UNINA Aerospace Propulsion Laboratory.

The test rig is a versatile set up primarily designed for testing hybrid rocket engines of several sizes and its sub-components. A detailed description of the laboratory and of the experimental facilities can be found in Ref. [17].

For the current research activities, novel, dedicated test set-up were developed to test the new high-performance UHTCMC materials in different configurations. Fig. 1 shows the design of the different proposed test articles. In particular, a first test campaign has been already successfully carried out to screen the most suitable materials candidates for the final applications, exposing small UHTCMC specimens to the supersonic exhaust jet of a 200N-class hybrid rocket nozzle [18, 19]. Based on these preliminary results, flat disks to be placed inside the hybrid rocket combustion chamber were manufactured and tested to assess the capability of larger components to withstand the considerable thermo-mechanical stresses expected inside the rocket without significant erosion. Then, nozzle-throat inserts and complete UHTCMC nozzles were tested to validate the technologies on samples having a shape and dimension close to the final application.

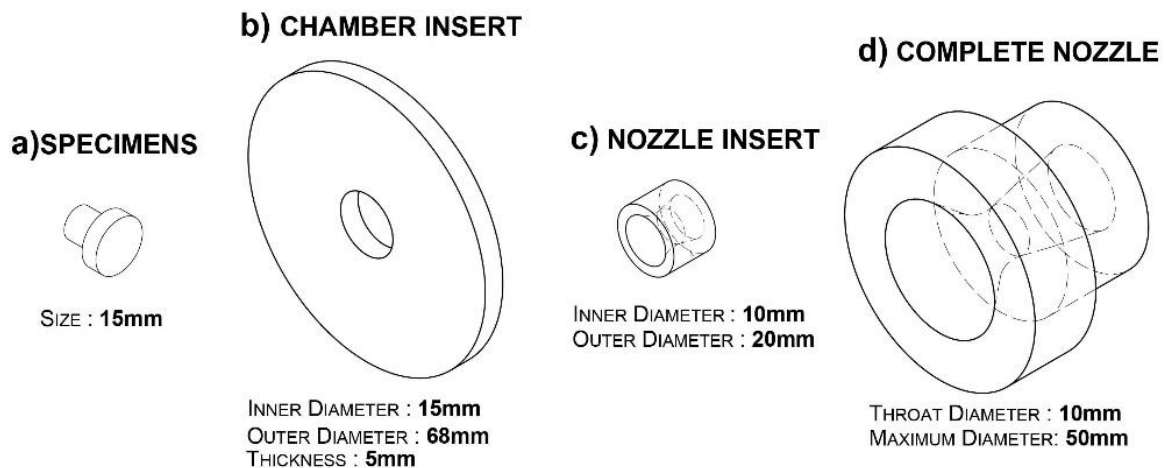


Fig. 1. Design of the test articles for material characterization for Hybrid Rocket Propulsion application.

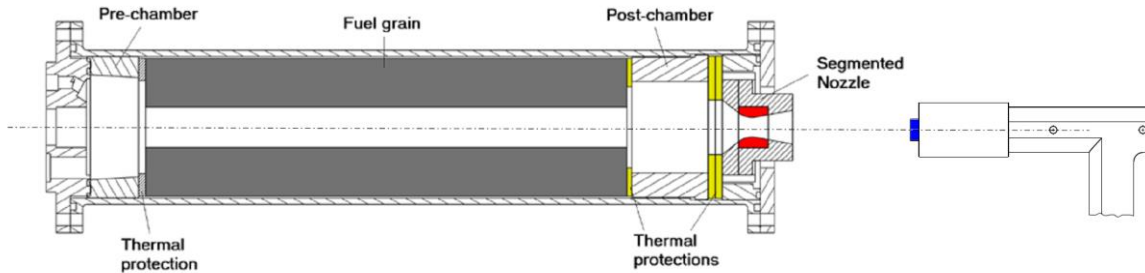


Fig. 2. Schematic section of the hybrid rocket and test setup for the different samples.

The schematics of the rocket employed in this work is depicted in Fig. 2, which also shows the UHTCMC sample (in blue) behind the rocket nozzle, the possible configuration for the chamber insert (in yellow) and the nozzle throat insert (in red). The tests presented in the following sections were performed with a converging nozzle injector, whose exit-section diameter is 6 mm, which delivered oxygen in single-port cylindrical fuel grains of HDPE. Oxidizer mass flow rate is controlled by means of a Tescom ER3000 pressure regulator, which controls an electropneumatic valve in order to reduce the feeding pressure to the desired setpoint, upstream a choked Venturi nozzle. The average fuel mass flow rate is estimated by means of grain mass measurements before and after the test (see Ref. [20]). Chamber pressure is measured by two capacitive transducers, Setra model C206, set up in the prechamber and in the aft-mixing chamber, while four load cells installed on the test bench allow thrust measurements. Finally, non-intrusive diagnostic equipment employed for the real-time evaluation of the sample surface temperature. In particular, the surface temperature of the samples can be continuously measured ($\pm 1\%$ instrumental accuracy) by digital two-color pyrometers (Infratherm ISQ5 and IGAR6, Impac Electronic GmbH, Germany) at an acquisition rate of 100 Hz.

2.1 Test conditions

Different test conditions have been selected, to evaluate the materials performance in different aero-thermo-chemical environments. All tests had a nominal duration of 10 s. Cylindrical 220mm-long HDPE grains were employed as fuel and gaseous oxygen as oxidizer.

In particular, two different set of test conditions have been considered, corresponding to an oxygen mass flow rate equal to 25 g/s and to 40 g/s, respectively. Only in the case of the free jet tests, in the former case, nozzles with 9.6 mm-initial diameter throat section have been employed, while a 12.5 mm-throat initial diameter nozzle has been used in the second case in order to have similar values of the chamber pressure, with a higher average oxidizer-to-fuel ratio, i.e. a more oxidizing chemical environment.

On the other side, for the other tests, two subsequent test have been performed, again with an oxygen mass flow rate equal first to 25 g/s and then to 40 g/s. In this case, for the estimation of the nominal test conditions the nominal value of the throat diameter, equal to 9.6 mm, has been considered.

Table 1 summarizes the main nominal operating parameters of the test conditions, as estimated by means of the numerical models described in [19].

Table 1. Summary of nominal time-averaged test conditions.

| | Test condition 1 | Test condition 2FJ | Test condition 2 |
|---|------------------|--------------------|------------------|
| Oxidizer mass flow rate [g/s] | 25 | 40 | 40 |
| Oxidizer-to-Fuel ratio | 5.13 | 6.50 | 6.50 |
| Chamber pressure [bar] | 6.49 | 5.65 | 9.63 |
| Combustion temperature [K] | ~ 3200 | ~ 3200 | ~ 3200 |
| Nozzle inlet CO ₂ mass fraction | 0.32 | 0.31 | 0.32 |
| Nozzle inlet H ₂ O mass fraction | 0.16 | 0.14 | 0.14 |
| Nozzle inlet O ₂ mass fraction | 0.30 | 0.41 | 0.41 |
| Nozzle exit pressure [bar] | 0.42 | 0.46 | 0.73 |
| Nozzle exit CO ₂ mass fraction | 0.36 | 0.34 | 0.39 |
| Nozzle exit H ₂ O mass fraction | 0.17 | 0.14 | 0.16 |
| Nozzle exit O ₂ mass fraction | 0.30 | 0.41 | 0.41 |

3. Experimental results

In this section, the results obtained for each step of the characterization campaign are presented and discussed.

3.1 Characterization of UHTCMC samples in free jet conditions

As mentioned before, the first step of the characterization of the new UHTCMC materials consisted in testing small samples exposed to the free jet of the exhaust gases coming from the hybrid rocket nozzle. Details about the different test performed can be found in [18, 19]. A synthesis of the most significant results, concerning test on the samples summarized in Table 2, is presented in the following. In particular, two samples had a Ti_3SiC_2 matrix with short (chopped) carbon fibers, uniformly dispersed into the matrix, and are referred to as TSC-SF. The other samples had the matrix based on ZrB_2 as major component and SiC as a minority phase. Two of them had long continuous carbon fibers, with a $0^\circ/90^\circ$ plies architecture, while the others had chopped fibers uniformly dispersed into the matrix.

Table 2. UHTCMC samples for free jet test.

| UHTCMC sample ID | Matrix composition | Carbon fibers |
|------------------|--------------------|---------------------------|
| TSC-SF-1 | Ti_3SiC_2 | Chopped |
| TSC-SF-2 | Ti_3SiC_2 | Chopped |
| ZBSC-SF-1 | ZrB_2/SiC | Chopped |
| ZBSC-LF-1 | ZrB_2/SiC | Continuous Unidirectional |
| ZBSC-LF-2 | ZrB_2/SiC | Continuous Unidirectional |

Samples TSC-SF-1 and ZBSC-LF-1 were tested in conditions 1, while samples TSC-SF-2, ZBSC-SF-1 and ZBSC-LF-2 were tested in conditions 2FJ.

Fig. 3 graphically represents the erosion rates of the different samples estimated on the basis of the mass loss. In both test conditions, ZrB_2/SiC -based specimens showed a better erosion resistance and structural behaviour with respect to Ti_3SiC_2 -based ones, while short-fibers and long-fibers ZrB_2/SiC -matrix samples showed a similar behaviour. In particular, sample ZBSC-LF-1 showed an excellent resistance to the less demanding test conditions to which it was subjected, preserving structural integrity and demonstrating an almost null erosion rate ($5 \cdot 10^{-4}$ mm/s), while sample TSC-SF-1 already showed a significant erosion rate, equal to 0.204 mm/s. On the other side, correspondingly to the harsher aero-thermo-chemical loads, although also the samples ZBSC-SF-1 and ZBSC-LF-2 showed a perceptible erosion rate (around 0.180 mm/s), it was anyhow significantly smaller than the case of sample TSC-SF-1, which was subjected to an erosion rate equal to 0.360 mm/s.

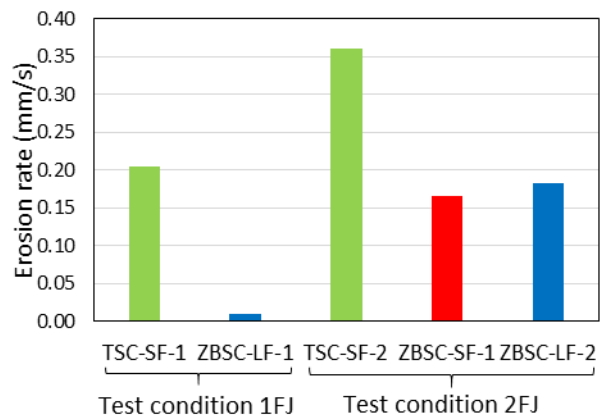


Fig. 3. Erosion rates of UHTCMC samples in free jet test

Fig. 4 shows the thermal histories of the samples detected by the pyrometer, while Fig. 5 and Fig. 6 respectively show pictures of the samples ZBSC-LF-1 and ZBSC-LF-2 after test, taken by a CCD camera and the optical microscope. It can be observed that, except for the case of the sample ZBSC-LF-1, all other samples experienced a sudden rise in temperature, which at the end of the test exceeded 2800 K. This jump might be associated to triggering, at high temperature, of chemical reactions involving the species contained in the ceramic matrix and/or the carbon fibers, which led to the formation of a porous and poorly-conductive oxidized phase, which for example is relatively small on sample ZBSC-LF-1 (Fig. 5) and is significantly more evident in case of ZBSC-LF-2 (Fig. 6). This oxide layer is characterized by low mechanical resistance and is therefore wiped out causing a significant material erosion.

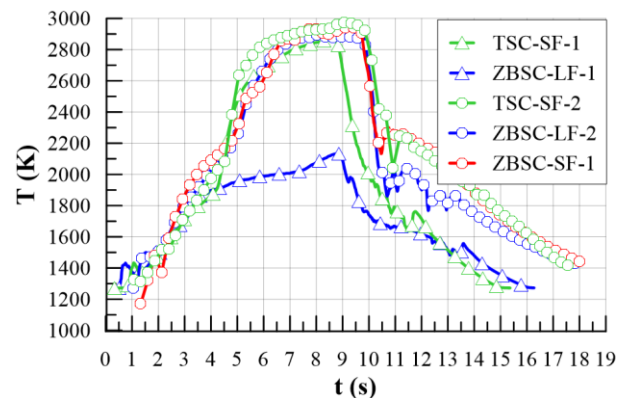


Fig. 4. Thermal histories of the samples in free jet test

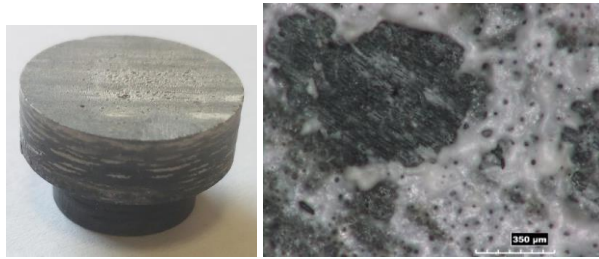


Fig. 5. Pictures of sample ZBSC-LF-1 after the test



Fig. 6. Pictures of sample ZBSC-LF-2 after the test

3.2 Test on UHTCMC flat disk chamber inserts

Based on the free jet test results, only ZrB_2 -SiC-based-matrix materials have been considered for the following steps of the experimental characterization campaign. Therefore, for the chamber insert tests, three flat disks with the matrix based on ZrB_2 as major component and SiC as a minority phase have been manufactured and tested. Two of them have long carbon fibers, but different level of the overall porosity, while the third sample have chopped fibers uniformly dispersed into the matrix. Finally, a classical C/SiC flat disk sample was tested as reference material. A summary of the chamber inserts tested is reported in Table 3.

Table 3. Chamber insert samples.

| Sample ID | Matrix composition | Carbon fibers | Porosity |
|-----------|--------------------|---------------|----------|
| C/SiC | SiC | Long | |
| CI-LF-1 | ZrB_2 /SiC | Long | < 1% |
| CI-LF-2 | ZrB_2 /SiC | Long | 15% |
| CI-SF-1 | ZrB_2 /SiC | Chopped | < 1% |

The chamber insert manufactured from the C/SiC flat plate has been tested subsequently twice, first in Test condition 1 and then in Test condition 2, referring to Table 1.

Fig. 7 shows the pictures of the sample before the test and after each test, where it is clearly observable the surface exposed to the flame and the enlargement of the transversal section, whose diameter increased from the initial value of 15 mm to a final value of around 20.6 mm after the two tests. Moreover, also for what concerns the structural resistance, although no cracks

were detected, the extreme conditions the material was subjected to determined a delamination of parts of the first layers, as it can be seen from Fig. 7c.

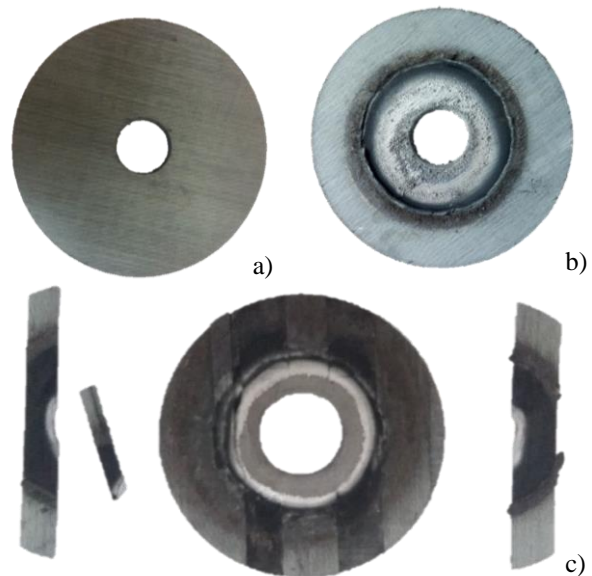


Fig. 7. Pictures of the C/SiC chamber insert: a) before test; b) after test 1; c) after test 2.

For what concerns the UHTCMC chamber inserts, three tests have been performed: CI-LF-1 chamber insert has been tested in Test condition 1, while CI-LF-2 and CI-SF-1 have been tested in Test condition 3.

Fig. 8, Fig. 9 and Fig. 10 show respectively pictures of the above-mentioned chamber inserts before and after test, from which it can be seen that CI-LF-1 and CI-SF-1 samples were subjected to structural cracks, which in the latter case, corresponding to the most severe test conditions, were fatal and led to leakage of the combusting gases determining critical damages also to the engine. Anyway, it is worth to note that, besides the zones around the crack, the internal surfaces of the hole do not show significant material erosion.

On the other side, CI-LF-2 chamber insert was not subjected to structural failure, as it can be seen in Fig. 9, and again no significant erosion has been measured



Fig. 8. Pictures of the CI-LF-1 chamber insert before and after test.



Fig. 9. Pictures of the CI-LF-2 chamber insert before and after test.



Fig. 10. Pictures of the CI-SF-1 chamber insert before and after test.

In conclusion, the results described above confirm the fact that the ZrB_2/SiC -based UHTCMC are characterized by outstanding erosion resistance, but a composite long-fiber architecture with sufficient porosity (around 15% in the present tests) is needed to obtain also sufficient structural resistance.

3.3 UHTCMC nozzle throat inserts test

Two UHTCMC nozzle throat inserts were manufactured and tested, which are summarized in Table 4. The two inserts had both a ZrB_2/SiC matrix, one with short (chopped) carbon fibers, uniformly dispersed into the matrix and the other with long continuous carbon fibers. Besides the UHTCMC throat inserts, a nozzle completely made of a classical commercial graphite has been tested in the same conditions as reference.

Table 4. UHTCMC nozzle throat inserts.

| Sample ID | Matrix composition | Carbon fibers | Porosity |
|-----------|--------------------|---------------|----------|
| TI-LF | ZrB_2/SiC | Long | 15 % |
| TI-SF | ZrB_2/SiC | Short | 5 % |

For the experimental characterization of each test article, two subsequent tests have been performed, again with an oxygen mass flow rate equal first to 25 g/s and then to 40 g/s, i.e. in test conditions 1 and 2 respectively.

After the first test in condition 1, it was detected that the throat diameter of the graphite nozzle increased from the nominal value of 9.6 mm to 9.9 mm, while no significant erosion occurred with the two UHTCMC throat inserts. After firing test in conditions 2, further considerable erosion occurred in the case of graphite nozzle, whose throat diameter increased up to around 11.4 mm. In the most severe conditions, also the TI-LF has been subjected to a perceptible erosion, which however was smaller than the former case, with an increase of the throat diameter up to 10.4 mm. On the other side, TI-SF showed a good resistance, with negligible erosion rate also at Test condition 2. The diagram in Fig. 11 graphically represents the corresponding average erosion rates, from which the improved resistance of the UHTCMC materials appears clear.

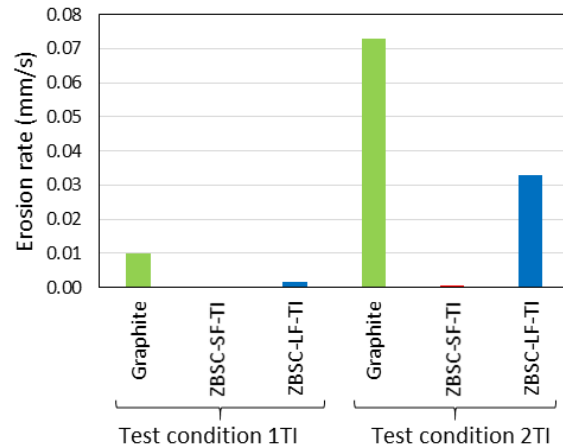


Fig. 11. Nozzle throat inserts erosion rates.

Fig. 12, Fig. 13 and Fig. 14 show the microscopic pictures of the zone around the throat section before tests and after both firing tests for the graphite nozzle, the TI-SF and TI-LF, respectively, from which the different growth of the throat section area can be observed. In the latter case, also an increase of the surface roughness can be noticed, probably due to the erosion of the carbon fibers which are less resistant than the ceramic matrix.

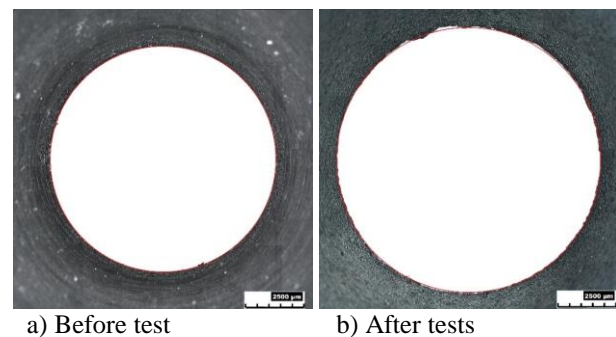
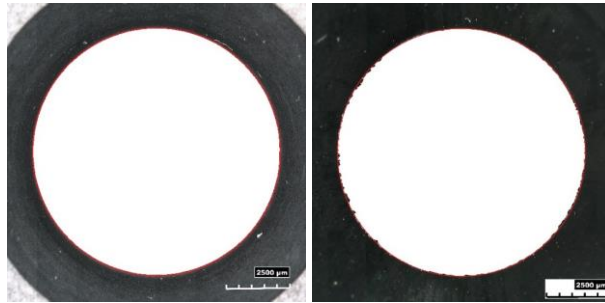
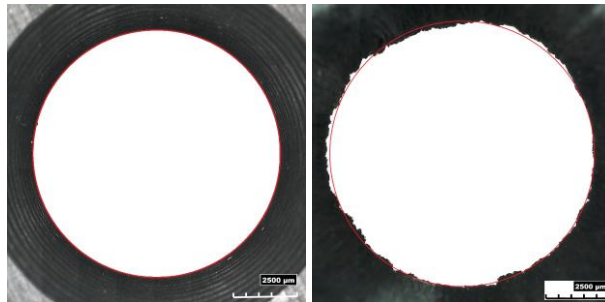


Fig. 12. Microscopic pictures of graphite nozzle throat.



a) Before test b) After tests
Fig. 13. Microscopic pictures of TI-SF nozzle throat.



a) Before test b) After tests
Fig. 14. Microscopic pictures of TI-LF nozzle throat.

The different erosion behaviour highlighted above affects directly the rocket performance. Fig. 15 shows the profiles of the measured chamber pressure during the operating time and the comparison with the corresponding theoretical pressure profile estimated with the tool described in [19], for the three firings performed in test conditions 2, in which the difference in the behaviours is more evident. In fact, in the test performed with the graphite nozzle the pressure trace shows a significantly decreasing trend due to the strong throat erosion. On the other side, in the test performed with the TI-SF, the chamber pressure is stable during the all engine operation, while, in the test performed with the TI-LF, the pressure trace is only slightly decreasing with respect to the numerically calculated one.

3.4 UHTCMC complete nozzles test

Finally, three complete UHTCMC nozzles have been manufactured and tested, which are summarized in Table 5. Again, they have a ZrB_2/SiC matrix, two with chopped fibers but different level of the overall porosity and the third one with long fibers.

Table 5. UHTCMC complete nozzles.

| Sample ID | Matrix composition | Carbon fibers | Porosity |
|-----------|--------------------|---------------|----------|
| CN-SF-1 | ZrB_2/SiC | Short | < 5% |
| CN-SF-2 | ZrB_2/SiC | Short | 10 % |
| CN-LF-1 | ZrB_2/SiC | Long | 5 % |

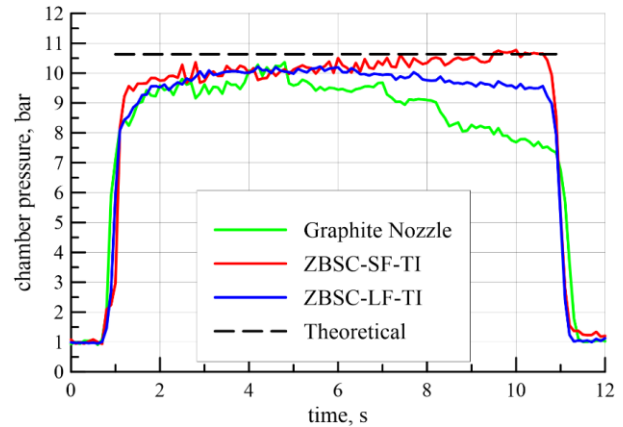
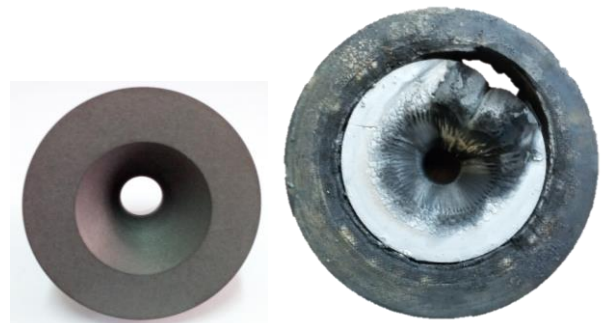


Fig. 15. Theoretical and measured chamber pressures vs operating time for tests in conditions 2.

Nozzles CN-SF-1 and CN-SF-2 have been both tested in test conditions 2 (see Table 1). As can be observed from Fig. 16 and Fig. 17 which respectively show picture of the two nozzles before and after test, although no significant throat erosion was detected in both cases, the nozzle CN-SF-1 characterized by a very low porosity was subjected to a structural failure. This failure led to leakage of the combusting gases, determining critical damages also to the engine and the consequential drastic reduction of the engine performance, as it can be observed for example from the pressure profile measured in the combustion chamber during the test shown in Fig. 18.



a) Before test b) After test
Fig. 16. Pictures of the CN-SF-1 nozzle.



a) Before test b) After test
Fig. 17. Pictures of the CN-SF-2 nozzle.

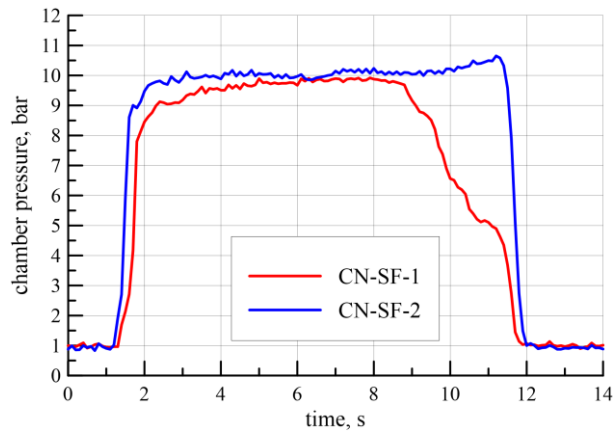


Fig. 18. Measured chamber pressures vs operating time for tests of nozzles CN-SF-1 and CN-SF-2.

As it can be observed in Fig. 19, the structural crack probably started from the sharp edge and propagated almost radially up to the throat section.



Fig. 19. Picture of the cut section of CN-SF-1 nozzle correspondingly to the radial crack.

On the other side, nozzle CN-SF-2 maintained structural integrity (Fig. 17) allowing a stable engine operation (Fig. 18), testifying once again that a sufficient porosity level could help improving the material resistance to mechanical and thermal loads.

Finally, three subsequent tests have been performed with nozzle CN-LF-1 in test conditions 2. Fig. 20 shows the pictures of the nozzle before and after each tests, while Fig. 21 shows the chamber pressure profiles during the tests. Once again, the long fibers architecture guaranteed outstanding performance in terms of both erosion and structural resistance, allowing a stable engine operation for a cumulative time of over 30 s.

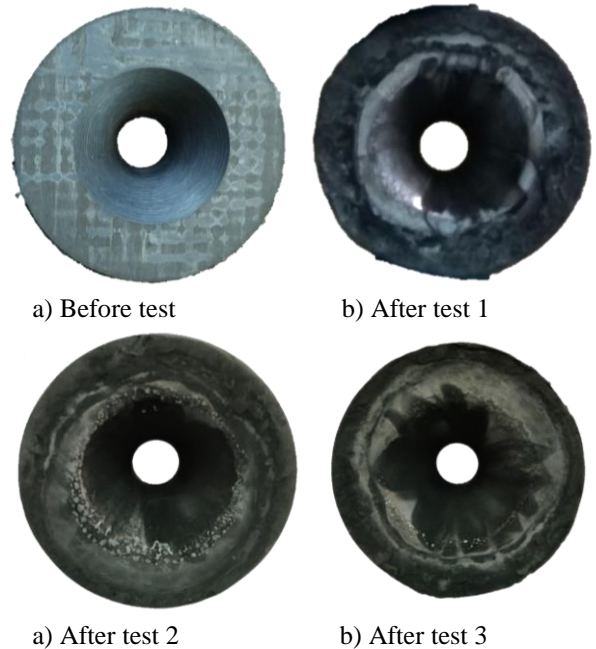


Fig. 20. Pictures of the CN-LF-1 nozzle.

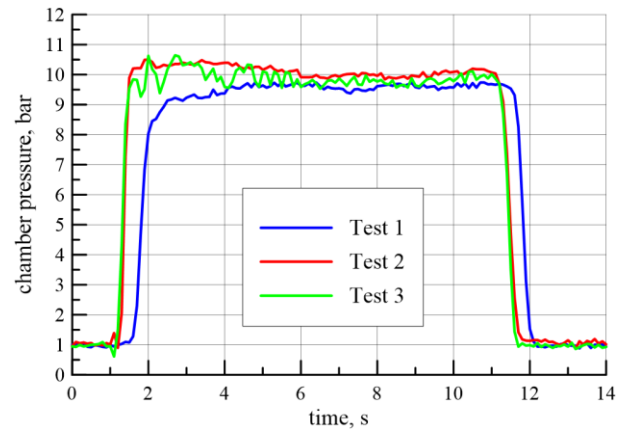


Fig. 21. Measured chamber pressures vs operating time for tests of nozzle CN-LF-1.

4. Conclusions

An extensive experimental campaign has been carried out for the characterization of a new class of UHTCMCs for near-zero erosion hybrid rocket nozzles. The test activities were structured according to an incremental approach, in different experimental configurations, with progressively increasing complexity and dimensions of the test articles. The first preliminary material screening activities, performed by exposure of small samples to the exhaust jet of a 200N-class hybrid rocket (free-jet test), identified ZrB₂-SiC composites with either short or long carbon fibers as the most promising candidates. It was also observed that when significant erosion occurred on UHTCMC samples, the material experienced also a sudden rise in temperature of several hundred degrees, reaching

temperatures up to 2800-2900 K, and solid fragments were wiped off the surface of the samples by the oncoming supersonic flow.

Subsequently, tests were carried out on flat disk inserts placed inside the rocket combustion chamber. This kind of test, besides confirming the outstanding erosion behaviour of ZrB₂/SiC-based materials, highlighted the fact that for samples with large size, a sufficient level of porosity (15 vol% in the specific case) is beneficial to withstand the thermo-mechanical loads, without any structural failures. Moreover, it was observed that long-fibers materials exhibited a better structural resistance.

ZrB₂/SiC-based nozzle throat inserts with short and long fibers were also tested in two increasingly demanding test conditions, showing again an excellent erosion resistance with respect to conventional graphite.

Finally, the most recent activities were carried out on subscale nozzles completely made of UHTCMCs, highlighting that long-fibers samples show the most promising behaviour, with no significant erosion nor structural failure even after repeated test sequences, whereas the mechanical performance of short fiber materials, despite an outstanding erosion resistance, is favoured by an optimized level of porosity.

Acknowledgements

The C³HARME research project has received funding by the European Union's Horizon2020 research and innovation programme under the Grant Agreement n° 685594.

The authors wish to thank Prof. Claudio Leone and Dr. Silvio Genna (CIRTIBS Research Center) for technical support in realizing the microscopic pictures of the samples.

References

- [1] G.D. Di Martino, S. Mungiguerra, C. Carmicino, R. Savino, Computational Fluid-dynamic Simulations of Hybrid Rocket Internal Flow Including Discharge Nozzle, AIAA 2017-5045, 53rd AIAA/SAE/ASEE Joint Propulsion Conference, 2017.
- [2] R. Savino, G. Festa, A. Cecere, L. Pienti, D. Sciti, Experimental Set Up for Characterization of Carbide-Based Materials in Propulsion Environment, *J. Eur. Ceram. Soc.* 35 (6) (2015) 1715-1723.
- [3] R. Hickman, T. Mc Kechnie, A. Agarwal, Net shape fabrication of high temperature materials for rocket engine components, AIAA 2001-3435, 37th Joint Propulsion Conference and Exhibit, 2001.
- [4] J.R. Johnston, R.A. Signorelli, J.C. Freche, Performances of rocket nozzle material with several solid propellants, NASA technical note 3428.3, 1966.
- [5] P. Thakre, V. Yang, Chemical erosion of carbon-carbon/graphite nozzles in solid-propellant rocket motors, *J. Propuls. Power* 24 (4) (2008) 822-833.
- [6] J.P. Murugan, T. Kurian, J. Jayaprakash, T. Jayachandran, Design and Thermo-Structural Analysis of the Interface between Subscale Versions of Carbon-Carbon (C-C) Nozzle Divergent to Metallic flange hardware for a Ground Simulation Test, IAC-17.C2.4.8, 68th International Astronautical Congress, Adelaide, Australia, 2017.
- [7] L. Kamps, S. Hirai, Y. Ahmimache, R. Guan, H. Nagata, Investigation of Graphite Nozzle-Throat-Erosion in a Laboratory-Scale Hybrid Rocket Using GOX and HDPE, AIAA 2017-4736, 53rd AIAA/SAE/ASEE Joint Propulsion Conference, 2017.
- [8] M. Natali, J.M. Kenny, L. Torre, Science and technology of polymeric ablative materials for thermal protection systems and propulsion devices: A review, *Progr. Mater. Sci.* 84 (2016) 192-275.
- [9] G.J.K. Harrington, G.E. Hilmas, Thermal conductivity of ZrB₂ and HfB₂, in: W. Fahrenholtz, E. Wuchina, W. Lee, Y. Zhou (Eds.), *Ultra-High Temperature Ceramics: Materials for Extreme Environment Applications*, 1st ed., John Wiley & Sons, Inc., 2014, pp. 197-235.
- [10] J. Koo, H. Stretz, J. Weispenning, Z. Luo, W. Wootan, Nanocomposite rocket ablative materials: processing, microstructure, and performance, AIAA 2004-1996, 45th AIAA/ASME/ASCE/AHS/ASC Structures, Structural Dynamics & Materials Conference, 2004.
- [11] D. Sciti, L. Zoli, L. Silvestroni, A. Cecere, G.D. Martino, R. Savino, Design, fabrication and high velocity oxy-fuel torch tests of a Cf-ZrB₂- fiber nozzle to evaluate its potential in rocket motors, *Mater. Des.* 109 (2016) 709-717.
- [12] Y. Wang, Z. Chen, S. Yu, Ablation behaviour and mechanism of C/SiC Composites, *J. Mater. Res. Technol.* 5 (2016) 170-182.
- [13] L. Zoli, D. Sciti, Efficacy of a ZrB₂-SiC matrix in protecting C fibres from oxidation in novel UHTCMC materials, *Mater. Des.* 113 (2017) 207-213.
- [14] L. Zoli, V. Medri, C. Melandri, D. Sciti, Continuous SiC fibers-ZrB₂ composites, *J. Eur. Ceram. Soc.* 35 (16) (2015) 4371-4376.
- [15] L. Zoli, A. Vinci, P. Galizia, C. Melandri, D. Sciti, On the thermal shock resistance and mechanical properties of novel unidirectional UHTCMCs for extreme environments, *Sci. Rep.* 8 (1) (2018) 9148.
- [16] R. Savino, L. Criscuolo, G.D. Di Martino, S. Mungiguerra, Aero-thermo-chemical characterization of ultra-high-temperature ceramics for aerospace applications, *J. Eur. Ceram. Soc.* 38 (8) (2018) 2937-2953.

- [17] G. D. Di Martino, C. Carmicino, R. Savino, Transient Computational Thermofluid-Dynamic Simulation of Hybrid Rocket Internal Ballistics, *J. Propuls. Power* 33 (2017) 1395-1409.
- [18] S. Mungiguerra, G. D. Di Martino, R. Savino, L. Zoli, D. Sciti, M.A. Lagos, Ultra-High-Temperature Ceramic Matrix Composites in Hybrid Rocket Propulsion Environment, AIAA 2018-4694, 2018 International Energy Conversion Engineering Conference, AIAA Propulsion and Energy Forum, Cincinnati, OH, July 2018.
- [19] G. D. Di Martino, S. Mungiguerra, A. Cecere, R. Savino, A. Vinci, L. Zoli, D. Sciti, Hybrid rockets with nozzle in ultra-high-temperature ceramic composites, IAC-18.C4.3.6x47333, 69th International Astronautical Congress, Bremen, Germany, 2017.
- [20] G. D. Di Martino, S. Mungiguerra, C. Carmicino, R. Savino, D. Cardillo, F. Battista, M. Invigorito, G. Elia, Two-Hundred-Newton Laboratory-Scale Hybrid Rocket Testing for Paraffin Fuel-Performance Characterization. *J. Propuls. Power* 35 (2019) 224-235.